

## A MONITORING SYSTEM FOR THE 60 MeV RADIOTHERAPY PROTON BEAM AT IFJ PAN USING A SCINTILLATING SCREEN AND A CCD CAMERA\*

M. BOBEREK<sup>1</sup>, J. SWAKOŃ<sup>1</sup>, L. STOLARCZYK<sup>1</sup>, P. OLKO<sup>1</sup>, M. WALIGORSKI<sup>1,2</sup>

<sup>1</sup> The “Henryk Niewodniczański” Institute of Nuclear Physics, Polish Academy of Sciences (IFJ PAN); ul. Radzikowskiego 152; 31-342 Kraków; Poland,

E-mail: marzena.boberek@ifj.edu.pl, jan.swakon@ifj.edu.pl, Liliana.stolarczyk@ifj.edu.pl, pawel.olko@ifj.edu.pl, z5waligo@cyf-kr.edu.pl

<sup>2</sup> “Maria Skłodowska-Curie” Memorial Institute, Centre of Oncology, Kraków Branch, Kraków, Poland

*Received April 23, 2013*

*Abstract.* A high-resolution system for imaging the transverse fluence distribution of a 60 MeV proton beam is under development at the Institute of Nuclear Physics of the Polish Academy of Sciences (IFJ PAN) in Krakow, Poland. This system will serve for quality assurance purposes in a proton ocular treatment facility. In the present system a highly efficient Gd<sub>2</sub>S<sub>2</sub>O:Tb scintillator (typically used in X-ray image converters), with maximum quantum efficiency around 550 nm, is applied to convert the ionizing proton beam to visible light. The light image of the beam is viewed by a sensitive ATIK 383 CCD camera of high spatial resolution (3362×2504 pixels) and further processed by dedicated software. To avoid radiation damage to the CCD sensor, the light from the scintillator is reflected by a glass mirror towards the camera. We report preliminary results of 2D proton beam fluence distributions obtained using our system and discuss its physical characteristics: linearity of light yield *versus* dose of proton beam.

*Key words:* proton beam radiotherapy, beam imaging, cross-section.

### 1. INTRODUCTION

Clinical application of passive beam scattering or of scanned proton pencil beam techniques in radiotherapy requires that precise localization and repeatability of the physical parameters of the beam be verified. In particular, accurate measurements of the dose distribution along the beam range (the per cent dose-depth – PDD) and across the beam axis (the dose profiles) at different beam depths are essential. Such measurements are part of the Quality Assurance (QA) system in

\* Paper presented at the 1<sup>st</sup> Annual Conference of the Romanian Society of Hadrontherapy (ICRSH 2013), February 21–24, 2013, Predeal, Romania.

radiotherapy, to enable precise and repeatable delivery of the beam dose to the tumour volume. To fulfil this requirement and to speed up the beam quality control procedure, a new system for proton beam spatial fluency imaging is under development. For a proton beam to be applied in ocular radiotherapy, the passively formed and collimated proton beam has to undergo a stringent Quality Control (QC) procedure. The required parameters of the pristine and spread-out proton beams have to be measured and maintained within pre-established tolerance levels. Among the controlled parameters are: transverse profiles of proton beam emittance, uniformity of dose and extent of lateral penumbra across the beam cross-section at different beam depths (ranges), and dose and distal fall-off along the beam range, for pristine and spread-out radiotherapy beams. Currently, these measurements are performed using a semiconductor diode scanned along and across the beam, which is a laborious and time-consuming process. To facilitate and speed-up this process, a new beam imaging system is under development at IFJ PAN. The new system consists of a beam-imaging scintillator, a high-resolution CCD camera, and dedicated data acquisition and image processing software. Results of preliminary tests of the prototype of this beam imaging system are reported here.

## 2. THE PROTON RADIOTHERAPY FACILITY

Proton beam irradiation of ocular melanoma patients is currently being performed at IFJ PAN [1, 2] using 60 MeV protons from the AIC-144 isochronous cyclotron [3]. The proton beam forming sequence consists of a single scattering foil, a range shifter and a range modulator. Additionally, a six-segment ionisation chamber is used for beam direction monitoring. Monitor chambers are used for dosimetry measurements. The final beam-forming elements are the snout and the collimator, manufactured individually for each patient (Fig. 1). During tumour irradiation, it is of primary importance to prevent any unnecessary movement of the eye-ball which contains the target volume. The prescribed dose is typically delivered in four fractions, over four consecutive days. To maintain fixed and repeatable positions of the patient's head and eyeball, an individual thermoelastic head mask is prepared and a fixed position of the eyeball achieved with the patient's active cooperation. Prior to patient exposure, the passively formed and collimated proton beam has to undergo a Quality Control (QC) procedure to verify the uniformity of dose and extent of lateral penumbra across the beam cross-section at different beam depths (ranges), and to verify the uniformity of dose and distal fall of along the beam range, against therapy planning calculations. Presently, such QC measurements are performed by scanning a semiconductor diode along and across the beam, a laborious and time-consuming process.

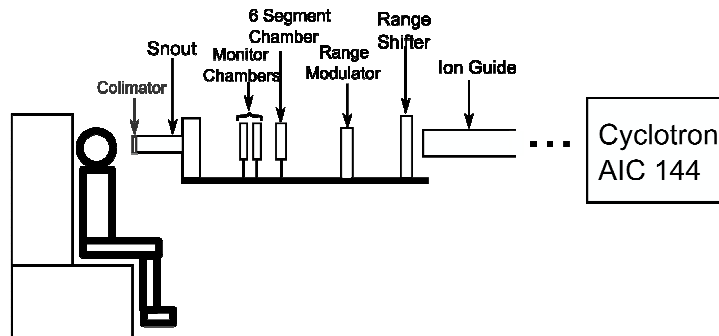


Fig. 1 – Scheme of the proton radiotherapy facility.

### 3. PROTON BEAM PROFILE IMAGING WITH SILICON DIODE

Beam profile imaging is the key step of beam QC. Presently, measurements are being performed by scanning the beam with a semiconductor diode. The beam profile scanner is mounted on the beam snout (Fig. 2). The active element of the profile scanner is a semiconductor diode, moved by a step motor, which measures the current induced by the beam. To measure vertical or horizontal transverse beam profiles, the scanner is rotated manually by 90 degrees.

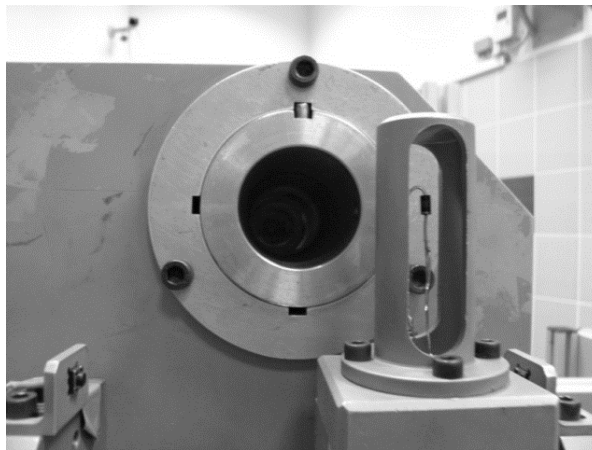


Fig. 2 – Profile Scanner with silicon diode.

A typical X (horizontal) profile measured by the present profile scanner is shown in Fig. 3. Measurement of a single one dimensional beam profile takes approximately 3 minutes. To accept the beam for therapy, a set of parameters needs to be calculated from the measured profile and lie within acceptance limits.

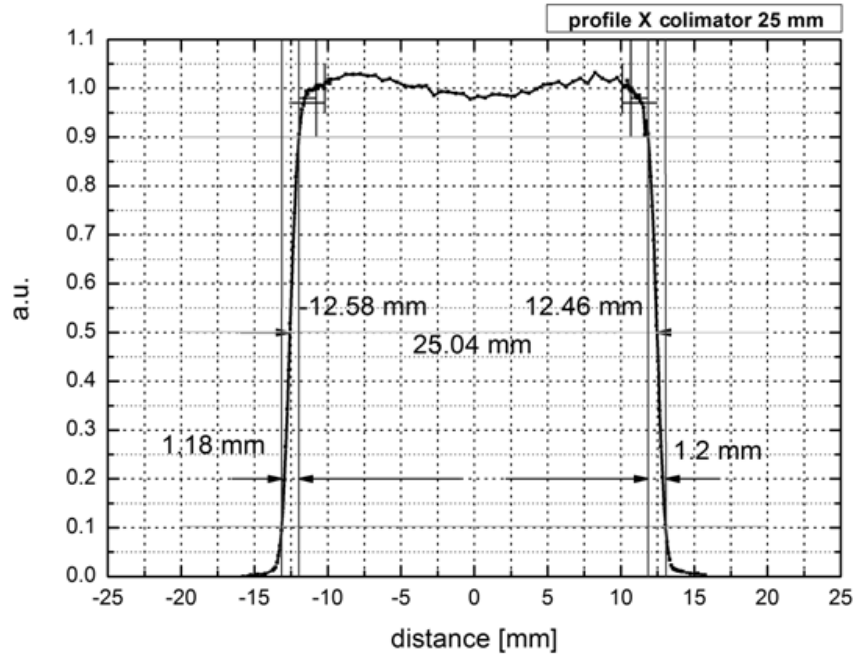


Fig. 3 – Result of the Profile Scanner measurements.

#### 4. DESIGN OF THE PROBIMS (PROTON BEAM IMAGING SYSTEM)

The main objective for developing the new beam QC system is to speed up the QA process by achieving two-dimensional imaging of the proton beam cross-section over the full range of depths, by using more sophisticated recording and data transfer techniques compared to those currently used. Our prototype system consists of a  $\text{Gd}_2\text{O}_2\text{S:Tb}$  (Gadolinium Sulphate Oxide doped with Terbium) scintillator [4] to efficiently convert the passage of protons of the beam through the scintillator to visible light pulses, and of a sensitive ATIK 383 CCD camera of high spatial resolution ( $3362 \times 2504$  pixels), able to record the 550 nm light emitted by the proton-irradiated scintillator. Modern CCD cameras offer high resolution imaging in visible-light wavelength range with a greyscale level of up to 16 bits. The general layout of the system is presented in Fig. 4.

To avoid radiation damage to the CCD camera sensor from protons in the beam, the camera is positioned perpendicularly to the beam axis and light from the scintillator is reflected by a 45-degree glass mirror. To achieve relatively high temporal resolution, data acquisition system based on the standard USB transfer is employed. The acquired images undergo detailed analysis in order to extract the physical and geometrical parameters of the beam. Prototype in-house developed

software for image analysis is being developed in MATLAB programming environment. The specific functions and algorithms are then transferred to the NI LabVIEW environment.

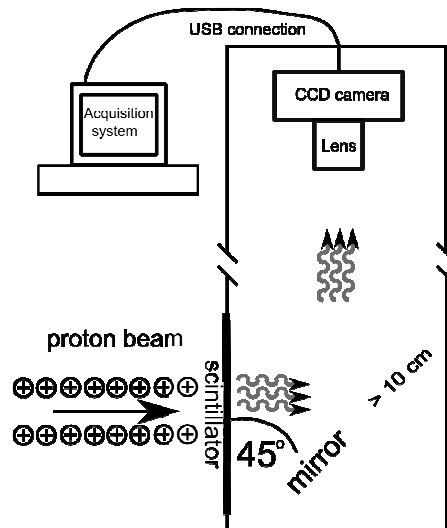


Fig. 4 – Layout of the beam scanning system.

## 5. REQUIREMENTS OF THE PROBIMS

The most important elements of the beam imaging system are the CCD camera and the scintillating screen. The requirements which the scintillator should fulfil for its application in the system, are [5, 6]:

- the scintillation spectrum and CCD sensor spectral sensitivity should be matched (350–550 nm range);
- the scintillator should be as thin as possible (no thicker than 2 mm) so as not to markedly affect the range of the proton beam. Moreover, self-absorption phenomena of visible light in the scintillator volume can strongly limit its light efficiency and narrow the light intensity range recorded by the CCD camera;
- high scintillation efficiency is necessary, to gather an image of sufficient intensity over a reasonably short exposure time. A sufficiently high density of scintillation centres should assure that an adequate number of scintillation events is recorded during proton beam imaging;
- scintillation efficiency should be a linear function of ionizing particle energy, enabling proton energy fluence distributions to be measured;
- the scintillator should not be too expensive, due to the limited budget of the project.

So far, we have examined the Gadolinium Sulphate Oxide doped with Terbium ( $\text{Gd}_2\text{O}_2\text{S:Tb}$ ) as the scintillating screen. This material was chosen for the prototype version of our system since its characteristics are well known and it is commonly used as an intensifying screen in X-ray cassettes. We are planning to examine the performance of another type of scintillator, namely PERLUX.

## 6. PRELIMINARY RESULTS

Preliminary results of ProBImS have been obtained for the 60 MeV proton beam generated using the AIC144 isochronous cyclotron.

### 6.1. BACKGROUND LEVEL OF THE $\text{Gd}_2\text{O}_2\text{S:Tb}$ SCINTILLATOR

In the prototype system the  $\text{Gd}_2\text{O}_2\text{S:Tb}$  scintillator was used. Preliminary measurements of this scintillator allowed us to evaluate its applicability in the system under development. The background level of the  $\text{Gd}_2\text{O}_2\text{S:Tb}$  screen varies with the dose absorbed in the scintillator, resulting in non-linearity of its dose response. Figure 5 presents background CCD signal intensity as a function of absorbed dose. The background signal intensity is the response of the CCD camera in the scintillator area (ROI – Region Of Interest) to which a given absorbed dose has been delivered.

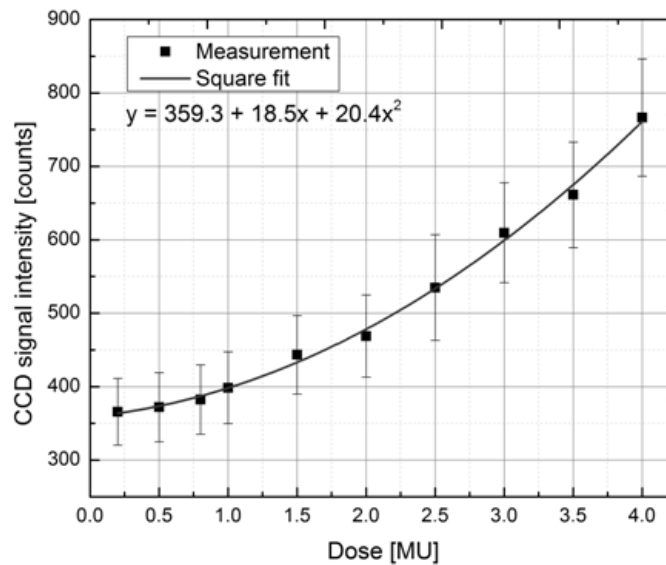


Fig. 5 – Background level as a function of absorbed dose.  
The available CCD signal intensity range is 0-65536.

Each value is calculated as the most probable pixel readout value (*i.e.* the argument of the maximum of best-fitted Gaussian to the histogram of pixel values over the ROI). Each point represents light intensity after irradiation with the dose unit, the dose being measured by the Monitor Ionization Chamber. The measurements were taken immediately after scintillator exposure to the proton beam. While the background level should be a linear function of the dose, a second-order polynomial best fits the measured data. This entails an unwanted apparent increase of the measured dose, as the abnormally high background (light intensity induced by the dose deposited in the scintillator) would contribute to dose measurement [7, 8]. This nonlinearity makes reliable measurements over the Bragg peak or the spread-out Bragg peak impossible. Thus, the  $\text{Gd}_2\text{O}_2\text{S:Tb}$  (the only scintillator examined so far), does not meet the requirements of the developed system. It is necessary to investigate other types of scintillators to find the most suitable one. Among candidates to be considered are: Thallium doped caesium iodide ( $\text{CsI:Tl}$ ), calcium tungsten-based intensifying screens (type PERLUX Universal, models: 28868UH, 28868UV, UH060478, UV 060478), rare earth-doped intensifying screens (type PERLUX, models: 752213, 851260) or plastic scintillators (type BC404 and BC408).

## 6.2. BEAM SPATIAL DISTRIBUTION

The beam imaging system under development will allow on-line control of the spatial stability of the beam. Figure 6 shows the 2-dimensional beam fluence distribution recorded with the new system, using the  $\text{Gd}_2\text{O}_2\text{S:Tb}$  scintillator. This is an example of preliminary measurement results, showing the enormous step forward compared to the 1-D profile scanning result of diode measurements. The camera raw output data is a 2-D grayscale image (Fig. 6d). To facilitate analysis, the grayscale was software-converted to a colour image (Fig. 6a – colours visible as various shades of gray). Lateral profiles over any beam intersection plane (such as the ones presented in Fig. 6b,c, corresponding to vertical and horizontal white lines in Fig. 6a) can be extracted from such images. The plotted profiles can be used for calculating the set of parameters corresponding to those extracted from silicon diode measurements.

## 6.3. BEAM PROFILE COMPARISON

Figure 7 presents the superimposed profiles obtained using Profile Scanner with silicon diode (black) and by CCD camera (gray). Presented profiles are slightly different. This may be caused by the scattering phenomenon of the charged beam particles on the scintillator material.

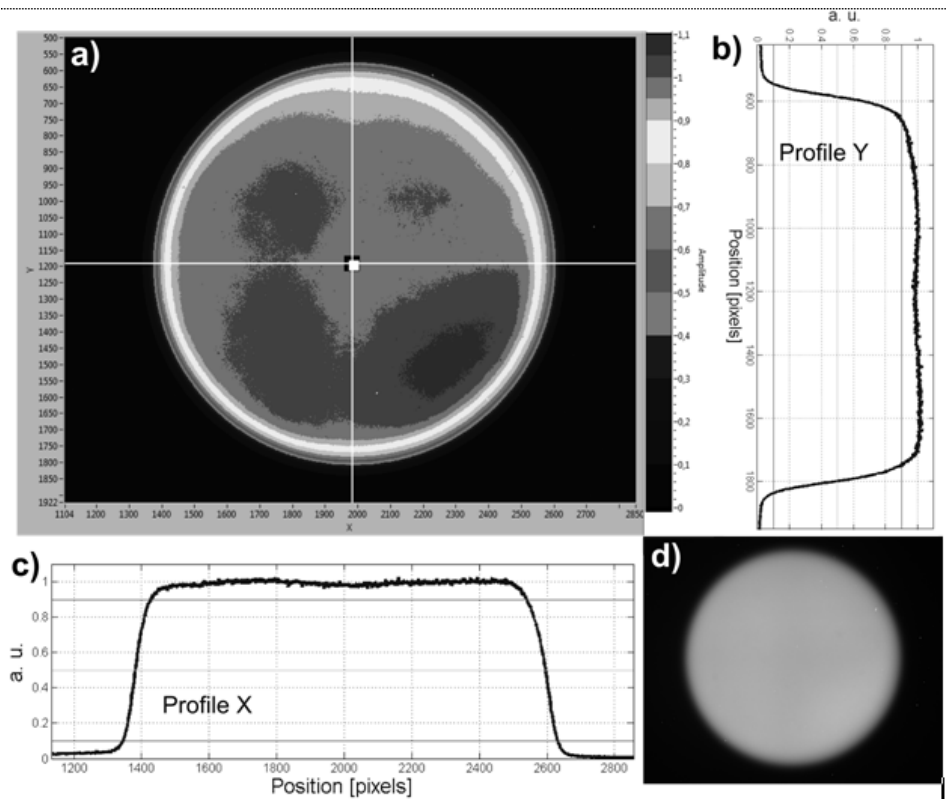


Fig. 6 – a) 2-dimensional beam spatial distribution recorded with the new system, using the  $\text{Gd}_2\text{O}_2\text{S:Tb}$  scintillator; b) vertical cross-section; c) horizontal cross-section; d) raw grayscale image of the beam.

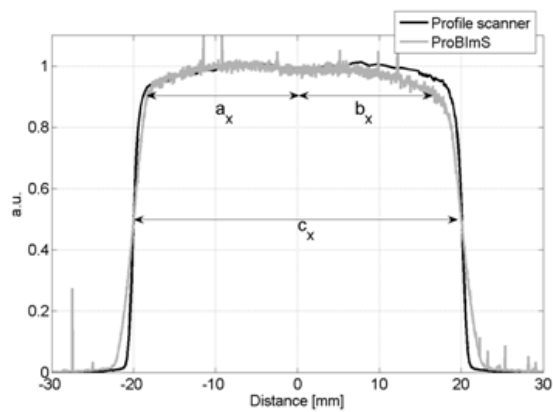


Fig. 7 – Profiles acquired *via* Profile Scanner with silicon diode (black) and ProBImS (gray).  
a.u. – arbitrary units.

In Table 1 a list of the obtained profile parameters is given. The widths of the penumbra calculated from profiles obtained using ProBImS are larger than those obtained from silicon diode measurements, which we attribute to scattering of radiation in the scintillator material.

*Table 1*

Comparison of the profile parameters gathered from profiles recorded with silicon diode scanner and ProBImS

	<i>Profile Scanner</i>	<i>ProBImS</i>
Left Penumbra (10÷90) [mm]	1.76	2.06
Right Penumbra (10÷90) [mm]	2.86	3.85
Symmetry on 90% level [%]	6.64	6.35
Field Ratio on 90% level [%]	0.94	0.91

As for the symmetry on 90% level the difference between ca. 6.64% and 6.35% is considered to be insignificant. The Field Ratios for both systems are comparable.

Symmetry at 90% level is calculated as the absolute value of the difference of  $a_x$  and  $b_x$  distances (Fig. 7) divided by the total profile width at 90% level ( $a_x + b_x$ ) times 100%. Field Ratio on 90% level is calculated as the quotient of the sum  $a_x + b_x$  and the width at half maximum ( $c_x$ ).

## 7. MEASUREMENTS OF NON-SCATTERED PROTEUS C-235 PROTON BEAM

Just very recently we have successfully performed preliminary measurements of the proton beam from our newly installed Proteus C-235 cyclotron, within the National Hadron Therapy Centre project at the IFJ PAN. The Proteus C-235 cyclotron is a variable-energy accelerator, delivering protons of energy up to 230 MeV. The new ocular beam will deliver protons of about 70 MeV. Treatment of all sites will be possible using the full beam energy and a scanning beam gantry.

Using the ProBImS prototype we recorded images of the non-scattered proton beam of the new cyclotron. The system allows precise positioning of the beam and helps in locating ionizing chambers for dose measurements. Moreover, the 2-D beam cross-sections, unavailable with currently used silicon diode scanners can now be recorded within 10 seconds. The first practical implementation of ProBImS was to evaluate the beam shape and direction measurements at the isocenter (at about 180 cm from the end of Ion Guide) and close to the Ion Guide (at about 2 cm). The energy of the beam was 70 MeV.

In Fig. 8a we present the raw data recorded with ProBImS, and Fig. 8b a three dimensional reconstruction of proton radiation intensity, recorded at 215 cm from the end of Ion Guide. The energy of the beam was 70 MeV.

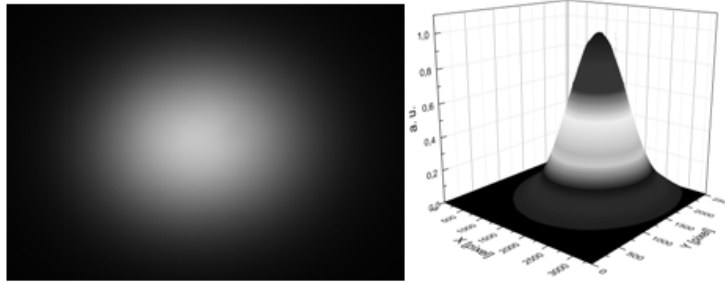


Fig. 8 – Image presented raw data recorded with the ProBImS (left) and a three dimensional reconstruction of the proton radiation intensity (right).

Figure 9 presents the 1-D profile extracted from the raw data presented in Fig. 8a. As we could see previously it is possible to extract detailed parameters of the beam, namely the symmetry and evaluate the shape of its cross-sections. The shape of the cross-section of beam intensity image can be represented by a Gaussian function (Fig. 9, black line).

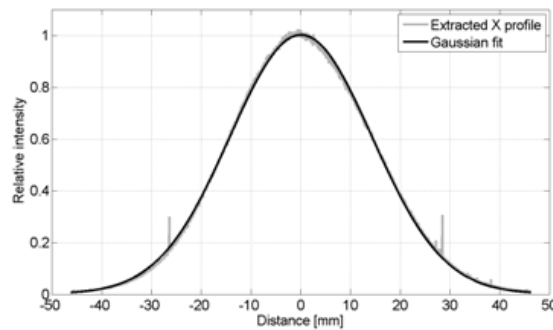


Fig. 9 – Profile X extracted from the acquired image of the non-scattered beam (gray line) and its Gaussian fit (black line). The distance from the ion guide to the scintillator screens was 215.1 cm.

## 8. CONCLUSIONS

The beam imaging system under development will allow on-line control of the spatial stability of the beam. It is expected that beam parameters will be calculated more rapidly (2-D intensity distribution of the entire beam cross-section within up to 10 seconds, against the present single 1-D profile obtained within 3

minutes). Data transfer from the CCD camera is efficient by employing USB bus. Lateral profiles over any beam intersection plane can be drawn from the images. ProBImS allows better quality of spatial fluence imaging to be achieved. This is an important element of the Quality Assurance System, through which the highest medical standards are maintained by precise evaluation of the physical characteristics of the radiotherapy proton beam.

*Acknowledgments.* This work has been supported by The EU Human Capital Operational Program, Polish Project No. POKL.04.0101-00-434/08-00 and The grant of the National Science Centre No. DEC-2011/01/B/ST2/02450.

## REFERENCES

1. J. Swakoń, P. Olko, D. Adamczyk, T. Cywicka-Jakiel, J. Dabrowska, B. Dulny, L. Grzanka, T. Horwacik, T. Kajdrowicz, B. Michalec, T. Nowak, M. Ptaszkiewicz, U. Sowa, L. Stolarczyk, M.P.R. Waligórski, *Radiat. Meas.*, **45**, 1469 (2010).
2. B. Michalec, J. Swakoń, U. Sowa, M. Ptaszkiewicz, T. Cywicka-Jakiel, P. Olko, *Appl. Radiat. Isotopes*, **68**, 738 (2010).
3. E. Bakewicz, K. Daniel, H. Doruch, J. Sulikowski, R. Taraszkiewicz, N. A. Morozov, E.V. Samsonov, N. G. Shakun, S. B. Vorojtosov, *Nukleonika*, **46**, 51 (2001).
4. E.I. Gorokhova, V.A. Demidenko, S.B. Mikhrin, P.A. Rodnyi, C.W.E. van Eijk, *IEEE T. Nucl. Sci.*, **52**, 3129 (2005).
5. G. A. P. Cirrone, G. Cuttone, D. Giove, P. A. Lojaco, R. Messina, A. Piemonte, *IEEE*, **3**, 1752 (2004).
6. G. A. P. Cirrone, S. Coco, G. Cuttone, C. De Martinis, D. Giove, P. A. Lojaco, M. Mauri, R. Messina, *IEEE*, **51**, 1401(2004).
7. J.W. Kwon, HJ Ryu, WH Ha, JK Lee, *J. Korean Phys. Soc.*, **48**, 759 (2006).
8. D.W. Kim, Y. K. Lim, J. Shin, S. Ahn, D. Shin, M. Yoon, S. B. Lee, *J. Korean Phys. Soc.*, **55**, 702 (2009).